Sensors & Transducers, Vol. 184, Issue 1, January 2015, pp. 60-65

www.sensorsportal.com

Sensors & Transducers

http://www.sensorsportal.com

Numerical Model of Piezoelectric Lateral Electric Field Excited Resonator

[1] Andrey TEPLYKH, [1] Boris ZAITSEV, [2] Iren KUZNETSOVA

[1] SB IRE nm. V. A. Kotelnikov RAS, Zelenaya 38, Saratov, 410019, Russia

[2] IRE nm. V. A. Kotelnikov RAS, Mokhovaya 11, bld. 7, Moscow, 125009, Russia

[1] Tel.: +7(8452)277323, fax: +7(8452)272401

E-mail: teplykhaa@mail.ru

Received: 14 November 2014 /Accepted: 15 December 2014 /Published: 31 January 2015

Abstract: Nowadays, piezoelectric lateral electric field excited resonators are frequently used for development of various acoustic sensors. But, the adequate theory of such resonators is absent. In this paper, the numerical method of calculation of characteristics of the acoustic oscillations in the piezoelectric lateral electric field excited resonators is developed. The developed method is based on the finite element analysis and allows computing the distribution of the components of the mechanical displacement in the piezoelectric plate and electric potential in the piezoelectric plate and surrounding vacuum at arbitrary frequency of the exciting field. This method allows setting various boundary conditions on various parts of a plate surface, including a condition of mechanical damping of oscillations. This allows calculating the frequency dependence of the real and imaginary parts of the electrical impedance/admittance of the resonator. We analyzed a piezoelectric lateral electric field excited resonator, which is based on a 0.5 mm-thick X-cut lithium niobate plate. Two infinitesimally thin metallic electrodes with width of 5 mm were deposited on top side of the plate. The electrodes were deposited in such a way that the lateral field was oriented along the crystallographic Y-axis. Calculations of electric impedance were carried out for various values of a gap in range 1 - 3 mm between electrodes. These results are in quantitative agreement with experimental data. A brief description of experimental set up is also presented. *Copyright © 2015 IFSA Publishing, S. L.*

Keywords: Acoustic resonator, Lateral exciting field, Finite element analysis, Lithium niobate.

1. Introduction

At present time researchers pay particular attention to the piezoelectric lateral electric field excited resonators because of development of various acoustoelectrical sensors. One of the main problems of the design of such devices is the suppression of undesirable acoustic oscillations and ensuring a high Q-factor of the resonator. Currently, this problem is solved experimentally by selection the optimal shape of the electrodes [1-2] or choosing the area of coverage of the damping coating [3-4]. However, such methods require a creation of a large amount of experimental samples. Researchers can theoretically estimate the efficiency of such resonators using the Christoffel - Bechmann method, which allows computing the electromechanical coupling coefficient for bulk waves excited by a lateral electric field [3-4]. However, this method does not take into account the finite aperture of the excited waves. Therefore, the problem of more accurate theoretical calculation of characteristics and efficiency of such resonators is

considered as urgent. In our previous work we introduce the numerical model of these resonators [5].

In this paper, we present a more detailed description of method for calculating the acoustic oscillations and the accompanying electric field in resonator representing a thin plate of a piezoelectric material with two rectangular electrodes on one side. The developed method is based on the finite element analysis and allows us to find the distribution of components of the mechanical displacement in the piezoelectric plate and electric potential in the piezoelectric plate and its surrounding vacuum at a certain oscillation frequency of the exciting field. This method takes into account the different boundary conditions on different areas of the resonator surface, and in particular, the mechanical damping of the parasitic oscillations, which was used in [1-2].

In Section 2, we give the description of the numerical model of resonator. In Section 3, we describe the experimental set up. In Section 4, we make the comparison of theoretical and experimental frequency dependencies of real and imaginary parts of electrical impedance of lateral electric field excited resonator. Finally, Section 5 presents the conclusions and the future research.

2. The Description of Numerical Model

In this paper, we consider a piezoelectric plate limited in x and y directions (Fig. 1). There are different boundary conditions on different parts of plate surface. Value of time-varying electric potential is given on an infinitely thin electrodes e1 and e2. The gap between electrodes is equal G. Special mechanical boundary conditions are specified on areas d1 and d2. The rest of plate surface is assumed mechanically and electrically free. In the z direction, the plate and electrodes assumed to be unlimited.

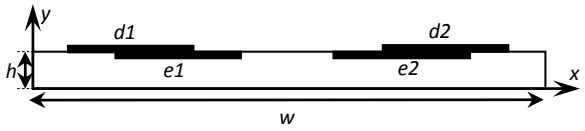

Fig. 1. The geometry of the problem.

So, we need to find a distribution of mechanical displacements within the plate, as well as the electric potential distribution inside the plate and in the surrounding vacuum.

As known, these distributions must satisfy inside the plate the motion equations:

$$\rho \frac{\partial^2 u_i}{\partial t_2} = c_{ijkl} \frac{\partial^2 u_l}{\partial x_j \partial x_k} + e_{kij} \frac{\partial^2 \varphi}{\partial x_j \partial x_k} \tag{1}$$

and the Laplace equation for piezomedium:

$$e_{jkl} \frac{\partial^2 u_l}{\partial x_j \partial x_k} - \varepsilon_{jk} \frac{\partial^2 \varphi}{\partial x_j \partial x_k} = 0 \tag{2}$$

Outside the plate, the distribution of electric potential should obey the Laplace equation for vacuum:

$$-\varepsilon_0 \nabla^2 \varphi = 0, \tag{3}$$

where, ρ is the piezomedium density, c_{ijkl}, e_{ijk}, and ε_{ij} are the tensors of elastic, piezoelectric and dielectric piezomedium constants, ε_0 is the dielectric permittivity of vacuum, u_i is the mechanical displacement component, φ is the electric potential, and indices $i, j, k, l = 1..3$, so $x_1 = x$, $x_2 = y$, $x_3 = z$.

Exciting electrical field is variable and is changed according harmonic law with frequency ω. Solution would be also harmonic because there are no other sources of excitation of oscillations and the problem is linear. Moreover the variable values are independent of coordinate z. This means that the following relations are valid:

$$\frac{\partial}{\partial t} = I\omega t, \qquad \frac{\partial}{\partial x_3} = 0,$$

where I is the imaginary unit, and mechanical displacement and electrical potential can be presented in the following form:

$$\left.\begin{aligned} u_i(x,y,z,t) &= u_i(x,y)\exp(I\omega t) \\ \varphi(x,y,z,t) &= \varphi(x,y)\exp(I\omega t) \end{aligned}\right\} \tag{4}$$

and, consequently, Eqs. (1-3) would be written as:

$$c_{ijkl} \frac{\partial^2 u_l}{\partial x_j \partial x_k} + e_{kij} \frac{\partial^2 \varphi}{\partial x_j \partial x_k} + \rho\omega^2 u_i = 0, \tag{5}$$

$$e_{jkl} \frac{\partial^2 u_l}{\partial x_j \partial x_k} - \varepsilon_{jk} \frac{\partial^2 \varphi}{\partial x_j \partial x_k} = 0, \tag{6}$$

$$-\varepsilon_0 \left(\frac{\partial^2 \varphi}{\partial x_1^2} + \frac{\partial^2 \varphi}{\partial x_2^2} \right) = 0, \tag{6}$$

where indices i, l = 1...3 and j, k = 1, 2. Thus, this problem is reduced to the following system of differential equations [6]:

$$L(u_i, \varphi) - f = 0, \tag{8}$$

where L is the differential operator and f is the unknown magnitude. So, the problem is to find (complex) values, i.e. magnitudes and phases of $u_i(x, y)$ and $\varphi(x, y)$ that satisfy Eqs. (5-7) with a given ω. One would solve this problem using the method of finite elements by deducing equations for elements

with the help of Galerkin's method. As shown in [6], the utilization of Galerkin's method combined with the method of finite elements results in the following system of equations:

$$\int_{\mathbf{R}} W_\beta \left(L(u_i, \varphi) - f \right) d\mathbf{R} = 0, \quad (9)$$

where **R** is the two-dimensional area, where solution must be obtained, and W_β is the system of basis (weight) functions. In order to account for the electric field distribution in space around the resonator, we surround the piezoceramic plate with some large-radius circular area and assume $\varphi = 0$ at the boundary of this area (Fig. 2).

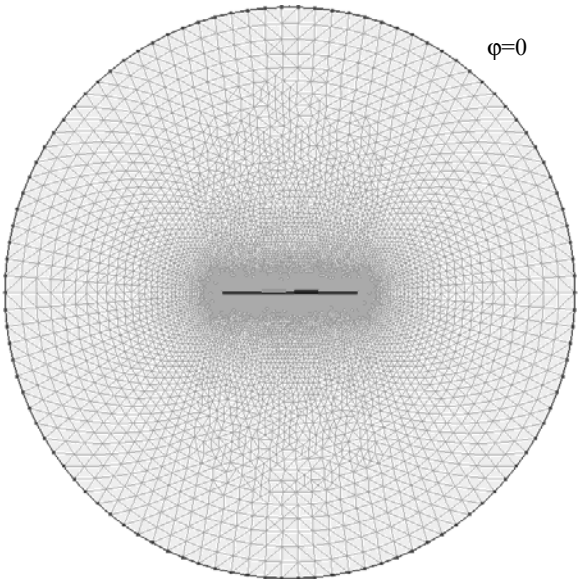

Fig. 2. General view of the **R** area divided into triangular elements.

For each element E corresponding to a triangle with vertices (X_p, Y_p)-(X_q, Y_q)-(X_r, Y_r), the function of element will be as follows

$$W_\beta^E = [a_\beta + b_\beta x + c_\beta y] \ (\beta = p, q, r)$$

or

$$\left.\begin{aligned} W_p^E &= [(X_q Y_r - X_r Y_q) + (Y_q - Y_r)x + (X_r - X_q)y]/2A \\ W_q^E &= [(X_r Y_p - X_p Y_r) + (Y_r - Y_p)x + (X_p - X_r)y]/2A \\ W_r^E &= [(X_p Y_q - X_q Y_p) + (Y_p - Y_q)x + (X_q - X_p)y]/2A \end{aligned}\right\}, \quad (10)$$

where p, q, r denote nodes forming element E, and A is the area of element E.

Substituting Eqs. (5-7) into Eq. (9) will yield the following system of equations which must be obeyed inside every element E from **R** inside the plate:

$$\int_E [W]^T \begin{pmatrix} \frac{\partial}{\partial x}\left(c_{i11l}\frac{\partial u_l}{\partial x} + c_{i12l}\frac{\partial u_l}{\partial y} + e_{1i1}\frac{\partial \varphi}{\partial x} + e_{2i1}\frac{\partial \varphi}{\partial y} \right) + \\ \frac{\partial}{\partial y}\left(c_{i21l}\frac{\partial u_l}{\partial x} + c_{i22l}\frac{\partial u_l}{\partial y} + e_{1i2}\frac{\partial \varphi}{\partial x} + e_{2i2}\frac{\partial \varphi}{\partial y} \right) + \\ \rho\omega^2 u_i \end{pmatrix} dE = 0', \quad (11)$$

$$\int_E [W]^T \begin{pmatrix} \frac{\partial}{\partial x}\left(e_{11l}\frac{\partial u_l}{\partial x} + e_{12l}\frac{\partial u_l}{\partial y} - \varepsilon_{11}\frac{\partial \varphi}{\partial x} - \varepsilon_{12}\frac{\partial \varphi}{\partial y} \right) + \\ \frac{\partial}{\partial y}\left(e_{21l}\frac{\partial u_l}{\partial x} + e_{12l}\frac{\partial u_l}{\partial y} - \varepsilon_{21}\frac{\partial \varphi}{\partial x} - \varepsilon_{22}\frac{\partial \varphi}{\partial y} \right) \end{pmatrix} dE = 0 \quad (12)$$

and in vacuum outside the plate:

$$-\int_E [W]^T \left(\frac{\partial}{\partial x}\left(\varepsilon_0 \frac{\partial \varphi}{\partial x} \right) + \frac{\partial}{\partial y}\left(\varepsilon_{22} \frac{\partial \varphi}{\partial y} \right) \right) dE = 0, \quad (13)$$

where T is the transposition operation,

$$u_i = W_p U_i^p + W_q U_i^q + W_r U_i^r,$$

$$\varphi = W_p \Phi^p + W_q \Phi^q + W_r \Phi^r$$

- are the interpolation polynomials for a two-dimensional triangle element E. The application of Galerkin's method requires the highest order of derivatives in Eqs. (11-13) to be not greater than by a unity above the order of continuity of the interpolation ratios used. That is why Eqs. (11-13) should contain derivatives of the order not higher than the first one. The application of procedure of lowering the order of derivations by integration by parts [6] will provide equations containing only unknown quantities and their first derivatives in the plate:

$$\left.\begin{aligned} &\int_E [W]^T \left(\rho\omega^2 u_i \right) dE - \int_E \frac{\partial [W]^T}{\partial x_j} \left(c_{ijkl}\frac{\partial u_l}{\partial x_k} + e_{kij}\frac{\partial \varphi}{\partial x_k} \right) dE + \\ &\int_B [W]^T \left(c_{ijkl}\frac{\partial u_l}{\partial x_k} + e_{kij}\frac{\partial \varphi}{\partial x_k} \right) n_j dB = 0 \end{aligned}\right\}, \quad (14)$$

$$\left.\begin{aligned} &\int_E \left(\frac{\partial [W]^T}{\partial x_j} \left(e_{jkl}\frac{\partial u_l}{\partial x_k} - \varepsilon_{jk}\frac{\partial \varphi}{\partial x_k} \right) \right) dE - \\ &\int_B [W]^T \left(e_{jkl}\frac{\partial u_l}{\partial x_k} - \varepsilon_{jk}\frac{\partial \varphi}{\partial x_k} \right) n_j dB = 0 \end{aligned}\right\} \quad (15)$$

and in vacuum:

$$\left.\begin{aligned} &\int_E \left(\frac{\partial [W]^T}{\partial x_j} \left(-\varepsilon_0 \delta_{jk}\frac{\partial \varphi}{\partial x_k} \right) \right) dE - \\ &\int_B [W]^T \left(-\varepsilon_0 \delta_{jk}\frac{\partial \varphi}{\partial x_k} \right) n_j dB = 0 \end{aligned}\right\}, \quad (16)$$

where B and n_j are the boundary of element and external normal to the boundary.

In order to ensure the unique solution of the equations system (14-16) we need to use boundary conditions. As for electrical boundary conditions they are standard for such types of problems [6]. At the boundary between the piezoplate and vacuum, excluding regions *e1* and *e2*, electrical boundary conditions consist in the continuity of electric potential and electric inductions components normal to the boundary:

$$\varphi^p = \varphi^v, \quad D_j^p n_j = D_j^v n_j, \tag{17}$$

where quantities with index p relate to the plate and those with v refer to vacuum. On the outside boundary Γ of the region **R** the potential is equal zero and on two electrodes it is assigned as following:

$$\varphi\big|_\Gamma = 0, \quad \varphi\big|_{e1} = +1, \quad \varphi\big|_{e2} = -1 \tag{18}$$

Mechanical boundary conditions are more difficult to formulate. A portion of the plate surface above the electrodes and around them was coated with absorbing varnish in the course of experiments with lateral field [1-2]. This was achieved to suppress undesired modes of oscillations of the plate and to increase the resonator's Q-factor. To reflect this fact in the theoretical model of resonator the mechanical boundary conditions were formulated as follows. The boundary condition at the surface of the piezoplate excluding regions *d1* and *d2* lies in the absence of normal components of mechanical stress and namely:

$$T_{ij} n_j = 0 \tag{19}$$

The boundary condition in regions *d1* and *d2* where damping coating is applied is written as follows:

$$T_{ij} n_j = i\omega Z_{ij} u_j, \tag{20}$$

where T_{ij}, n_j, Z_{ij} and u_j are the tensor of mechanical stresses of the piezoplate, normal to the surface, acoustic impedance of the coating and mechanical shift, respectively. This condition was obtained as generalization of the known relation [7] in the following form:

$$p = Zv, \tag{21}$$

where p and v are the acoustic pressure and oscillation rate, respectively, for boundaries between gas and liquid media and anisotropic solids. For $Z_{ij} \to 0$ this condition goes into the condition of free surface $T_{ij} n_j = 0$ and for $Z_{ij} \to \infty$ this condition goes into the condition of rigidly fixed surface $u_j = 0$. In the case under study $Z_{ij} = Z\delta_{ij}$, where Z is the acoustic impedance of varnish.

3. The Description of Experimental Setup

In order to compare the theoretical results with experimental data, the lateral electric field excited resonator on X-cut lithium niobate plate was made [2]. The scheme of this resonator is presented in Fig. 3. The shear dimensions and thickness of plate were equal 18×18 mm and 0.5 mm, respectively. Two 200 nm – thick aluminum rectangular electrodes with dimensions of 5×10 mm were deposited on one side of the plate through a special mask in vacuum. The electrodes were deposited in such a way that the lateral field was oriented along the crystallographic Y-axis (Fig. 3). This field component excited a longitudinal acoustic wave re-reflected between the plate sides with the largest electromechanical coupling coefficient [1]. The gap G between electrodes was equal to 1 mm. The area around the electrodes and part of electrodes with width of 3 mm were coated with a damping layer of absorbing varnish with thickness of about 0.2 mm.

The frequency dependences of the real and imaginary parts of electric impedance of resonator were measured using the LCR meter (4285A, Agilent Technologies Inc.). These dependences for pointed above resonator are presented in Figs. 5-7 by dashed lines.

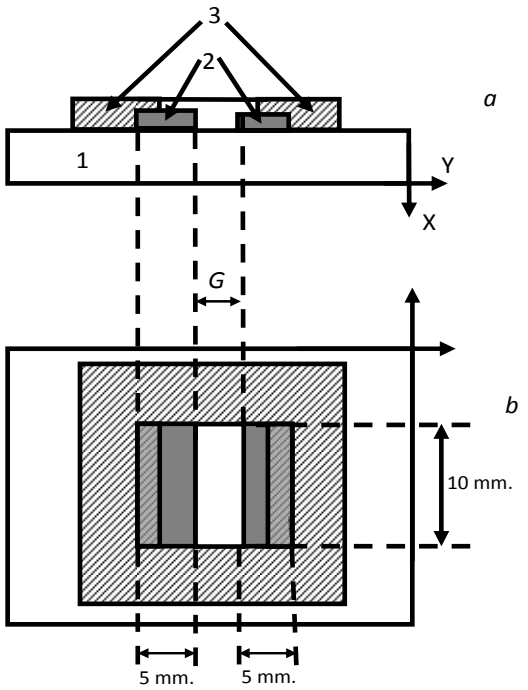

Fig. 3. The side (*a*) and top (*b*) views of the resonator with the lateral exciting electric field: X – cut lithium niobate plate - 1, electrodes - 2, and absorbing coating - 3.

4. The Comparison of the Theoretical and Experimental Results

In accordance with experiment, the calculation was performed for the case when the thickness h and

width w of the plate were equal to 0.5 mm and 18 mm, respectively (Fig. 1). On the upper surface of the plate, two electrodes e1 and e2 were deposited. The lateral electric field was oriented along the crystallographic Y-axis. The width of each electrode e1 and e2 was equal to 5 mm with the gap G between them in range 1 - 3 mm in different experiments. The width of damping regions d1 and d2 was of 5 mm and the regions of overlap (d1 - e1) and (d2 - e2) were fixed to 3 mm.

Since the above-described method of calculation allows us to find the distribution of all variables and their derivatives for any given frequency, it was possible to build electrical impedance depending on the frequency of this resonator and compare them with experiment. So, we calculated the distribution of the acoustic field and the electric potential in the range f = 6-7 MHz. It is clearly seen in Fig. 4 that the maximum amplitude of the acoustic vibrations are located in the gap between the electrodes. These oscillations correspond to the longitudinal bulk acoustic wave propagating in the vertical direction between the boundaries of the plate. This wave is the cause of deep resonance on frequency dependence of the electrical impedance [1-2] shown on Figs. 5-7.

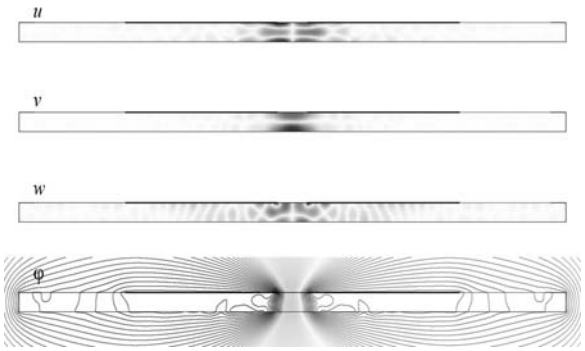

Fig. 4. Distribution of the components of mechanical displacement and electric potential in resonator excited by electric field at frequency 6.55 MHz.

The theoretical value of the impedance is calculated in accordance with the formula:

$$Z = (\varphi_2 - \varphi_1)/J, \tag{22}$$

where φ2 – φ1 is the potential difference between electrodes, J is the displacement current:

$$J = \int_S \frac{\partial D}{\partial t} ds \tag{23}$$

This integral is taken over the both top and bottom surfaces of the electrode. The calculated frequency dependencies of real and imaginary parts of electrical impedance are presented by solid lines in Figs. 5-7. The material constants of lithium niobate were taken from [8].

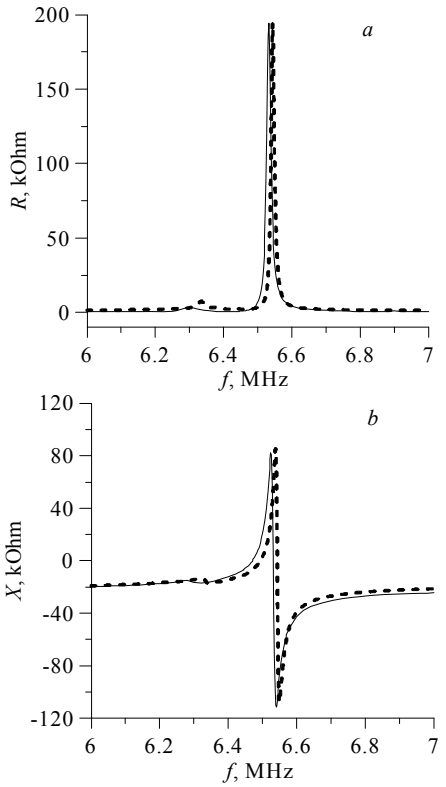

Fig. 5. Theoretical and experimental value of the real (*a*) and imaginary (*b*) components of the electrical impedance of the resonator with a 1 mm gap between the electrodes. Solid line is theory, dashed line is experiment.

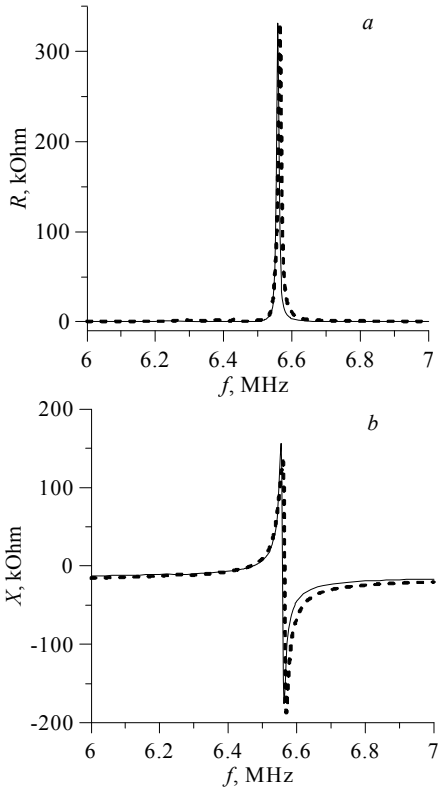

Fig. 6. Theoretical and experimental value of the real (*a*) and imaginary (*b*) components of the electrical impedance of the resonator with a 2 mm gap between the electrodes. Solid line is theory, dashed line is experiment.

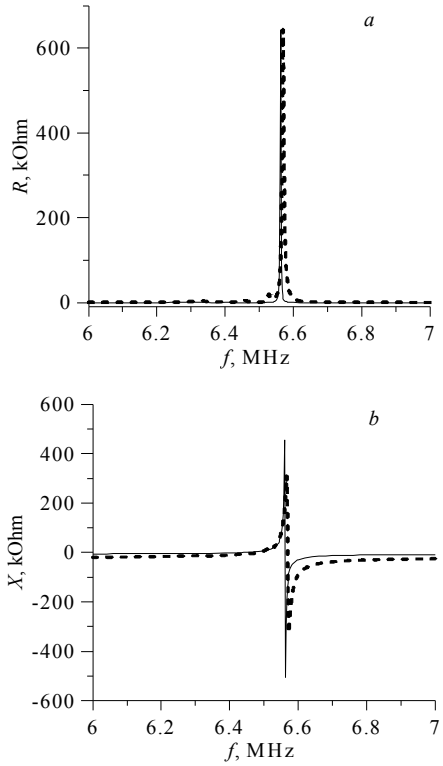

Fig. 7. Theoretical and experimental values of the real (*a*) and imaginary (*b*) components of the electrical impedance of the resonator with a 3 mm gap between the electrodes. Solid line is theory, dashed line is experiment.

One can see from Figs. 5-7 that a good agreement exists between theoretical and experimental dependencies. Therefore, the difference between values of resonant frequency does not exceed 15 kHz. A slightly bigger distinction in absolute values of X is explained by the parasitic electric capacity of the device, which has not been considered in calculation. Moreover, the used material constants taken from [8] may differ from actual ones in the range ±5 % (standard error for modern technology of crystal growing process).

5. Conclusions

The obtained results have shown the adequacy of the developed method for the characteristics calculation for resonators excited by a lateral electric field. These results will be used in future to develop sensors of fluid properties.

Acknowledgements

The work was financially supported by the grant of President of Russia MK-5551.2014.9.

References

[1]. B. D. Zaitsev, I. E. Kuznetsova, A. M. Shikhabudinov, A. A. Vasiliev, The research of the piezoelectric crystal resonators with the lateral field excitation, in *Proceedings of the IEEE Int. Ultrasonics Symposium*, 2010, pp. 946–949.

[2]. B. D. Zaitsev, I. E. Kuznetsova, A. M. Shikhabudinov, A. A. Teplykh, I. A. Borodina, The study of Piezoelectric Lateral-Electric-Field-Excited Resonator, *IEEE TUFFC*, 2014, Vol.61, No. 1, pp. 166-172.

[3]. D. F. McCann, J. M. McGann, J. M. Parks, D. J. Frankel, M. Pereira da Cunha, J. F. Vetelino, A Lateral-Field-Excited LiTaO3 High Frequency Bulk Acoustic Wave Sensor, *IEEE TUFFC*, 2009, Vol. 56, No. 4, pp. 779–787.

[4]. T. G. Leblois, C. R. Tellier, Design of new Lateral Field Excitation Langasite Resonant Sensors in *Proceedings of the IEEE Int. Ultrasonics Symposium*, 2009, pp. 2672–2675.

[5]. Andrey Teplykh, Boris Zaitsev, Iren Kuznetsova, Numerical Model of Piezoelectric Lateral Electric Field Excited Resonator as Basic Element of Acoustic Sensors, in *Proceedings of the 8th International Conference on Emerging Security Information, Systems and Technologies (SENSORDEVICES '14)*, Lisbon, Portugal, November 16-20, 2014, pp. 23-25.

[6]. L. Segerlind, Applied Finite Element Analysis. Second Edition, *John Wiley & Sons, Inc.,* 1984.

[7]. E. Skudrzyk, The Foundation of Acoustics: Basic Mathematics and Basic Acoustics, *Springer-Verlag*, 1971, pp. 396-400.

[8]. G. Kovacs, M. Anhorn, H. E. Engan, G. Visintini, C. C. W. Ruppel, Improved material constants for LiNbO3 and LiTaO3, in *Proceedings of the IEEE Ultrasonics Symposium*, Vol. 1, 1990, pp. 435-438.